Progress in Modeling the Impact of Land Use Change on the Global Climate

Haydee Salmun
Department of Geography
Hunter College of the City University of New York
New York, NY 10021
Tel: 212-772-5224
Fax: 212-772-5268
email: hsalmun@geo.hunter.cuny.edu

Andrea Molod
Department of Earth, Atmospheric and Planetary Sciences
MIT, Cambridge, MA 02139
email: molod@ocean.mit.edu

Manuscript submitted to Progress in Physical Geography

May 2005

Progress in Modeling the Impact of Land Use Change on the Global Climate

Abstract: The prediction of the impact of anthropogenic land use change on the climate system hinges on the ability to properly model the interaction between the heterogeneous land surface and the atmosphere in global climate models. This paper contains a brief review of techniques for modeling this interaction in General Circulation Models (GCMs) that have been used to assess the impact of land use change on climate, along with a summary of the physical mechanisms described by these simulations. Evidence exists which suggests that the vertical extent to which surface heterogeneities retain their individual character is an important consideration for the land-atmosphere coupling, and a recently developed technique that allows the character of the land surface to influence the atmosphere higher above the surface than other techniques in use is described. The differences in the simulated climate between this new technique and the technique in general use are discussed. This includes the presence of a boundary layer feedback mechanism that is not present in simulations with the standard technique. Simulations carried out with the new technique demonstrate that the coupling between land and atmosphere is strengthened in many regions. We postulate that the new technique when implemented in a GCM has the potential to affect and improve our predictions of the influence of anthropogenic land use change on climate.

Key words: Modeling, land-atmosphere interactions, land use change, climate change.

Introduction

The record of observed global surface air temperature over the past century indicates a clear warming trend for our planet, with the year 2001 being the second warmest on record (IPCC 2001). There is now evidence that the warming observed over the last 50 years is due in part to anthropogenic activities, including greenhouse gas emissions and land use change. Anthropogenic land use change (LUC) includes urbanization, deforestation, desertification and agricultural practices, all of which have been shown to have an important effect on climate and climate change (Pielke *et al*., 2002). Many observational studies have shown the impact of LUC on regional climate. For example, an analysis of observations has shown that urbanization and the associated heat island contribute regionally to the warming trend of the last 50 years over the US (Gallo *et al*., 1999), and that the contributions of urbanization and agricultural expansion combined account for as much as half of that trend (Kalnay and Cai, 2003). In addition, satellite observations show an increase in the seasonality of clouds and convection over the Amazon basin associated with deforestation (Durieux *et al*., 2003). Other observational studies show that the change in the Florida Everglades between 1900 and 1990 from wetlands and marsh to agricultural and urban terrain has been connected with a drier and warmer climate (Pielke *et al*., 1999), that the conversion of terrain in southwestern Australia has been associated with increased formation of cumulus clouds in that region (Ray *et al*., 2001), and that the deforestation of southern Spain since the middle ages is associated with a regional desertification and change in the regional hydrological regime (Millan *et al*, 2005). The evidence that anthropogenic activity is contributing to the warming trend is further supported by the fact that comparisons between observations and global model simulations of the evolution of the earth's climate over the period 1860-2000 show that the closest agreement between observed and simulated climate is obtained when the simulations include both natural and human factors. The simulations include the effects of the anthropogenic increase of greenhouse gases in the atmosphere as well as a rudimentary accounting for the effects of anthropogenic LUC.

Many simulations and studies of the effects of deforestation and overgrazing have been conducted using coarse resolution global models, and although they agree better with observations than simulations that do not include these effects, they still produce results that differ from high-resolution models and observations. In addition, the results are highly dependent on the specific land surface model formulation (Koster *et al*., 2002). A critical component of the land surface model formulation is the technique used to account for the fact that the surface underlying a General Circulation Model (GCM) grid box is heterogeneous in vegetation and soil properties. Properly capturing (parameterizing) the effects of this heterogeneity on the grid scale is crucial to the prediction of climate and climate change, and to the prediction of the effect of LUC on the changing climate.

The present article focuses on the manner in which information is communicated between the heterogeneous land surface and the overlying atmosphere. We begin with a brief review of the modeling techniques that are used to represent the aspects of the land-atmosphere exchange associated with small-scale heterogeneities in surface vegetation. These aspects directly affect the ability of a GCM to assess and predict the contribution of land use change to the observed temperature trend. Following this introduction we present a brief review of the techniques that are used in climate models for the coupling between the land surface and the atmosphere. GCM experiments conducted to assess the climate impact of deforestation and desertification, the most extensively studied forms of land use change, are discussed to summarize our current understanding of the mechanisms involved. The following section is devoted to a newly developed technique called 'Extended Mosaic' (EM) to couple the land surface and the atmosphere that has the ability to overcome some of the limitations of other existing techniques. This section includes a review of a GCM study that showed the impact of using EM on the local boundary layer structure, thereby on the regional climate, and a discussion of new calculations which show that the strength of the land-atmosphere coupling is affected by the choice of modeling technique. In the final section, we discuss the implications of this new development for modeling the impact of land use change on regional and global climate and offer a perspective on how land surface processes might be more realistically and accurately calculated in the next generation of coupled models used for climate studies.

II. GCM Studies of the Effects of land Use Change

1 Parameterizations of Land-Atmosphere Coupling

The elements in a GCM that handle the land-atmosphere interface are the surface layer and boundary layer models, the land surface model, and the technique used to couple them. The surface and boundary layer models involve parameterizing near surface turbulence as a diffusive process (Randall, 2000), and the land surface model parameterizes the surface and sub-surface mass and energy transfers. A comprehensive review of the development of land surface models over the past forty years can be found in Pitman (2003). The focus of the present article is the techniques used for the coupling between the land surface and the atmosphere.

The calculation of the land-atmosphere exchange in global climate models, as well as the prediction of the potential impact on climate of land use change, is complicated by the fact that the character of the land surface is highly variable. Vegetation cover, the types of terrain, soil texture and wetness, the amount of cloud cover and precipitation, and the extent of urban areas all contribute to land surface variability. The wide range of scales of variability in the land surface is apparent in the global vegetation maps that have been compiled from visible and other imagery. The scale of these heterogeneities may be smaller, and in some cases much more so, than the characteristic grid scale in most current GCMs used in climate studies (on the order of 200 km). Almost all the Soil-Vegetation-Atmosphere-Transfer (SVAT) models that are coupled to state of the art regional and global climate models employ some technique to attempt to account for the subgrid-scale heterogeneities. The most often used techniques are 'dominant', 'composite' and 'mosaic' and they are briefly discussed here. Figure 1 shows a schematic view these different techniques. The top panel of the figure depicts a hypothetical grid square with four characteristic vegetation types and some known geographical distribution. The bottom panels depict the same grid square as 'seen' by the atmosphere in a GCM when the three different techniques are implemented to describe the land surface.

The earliest of the SVAT formulations for GCMs assumed that the land surface in a GCM grid square can be adequately described by the soil and vegetation characteristics of the region that occupies the majority of the area in a grid box (Dickinson *et al*., 1986). This 'dominant' technique cannot, however, account in any way for the influence of other vegetation and soil types that may exist over significant areas of the grid box (see the panel named 'dominant' in figure 1). Many of the GCMs that are participating in the Atmospheric Model Intercomparison Project (AMIP) II (Gates, 1995) account for the subgrid-scale variability by specifying soil and vegetation parameters that represent a homogeneous 'composite' vegetated surface and its underlying soil for each GCM grid square. Among these are the GCMs used at the ECMWF (Viterbo and Beljaars, 1995), NCAR (Gates, 1995), NCEP (Pan and Mahrt, 1987), the Center for Ocean-Land Atmosphere Studies (Xue *et al*., 1991), the Canadian Climate Centre (Verseghy *et al*., 1993), and Météo-France (Mahfouf *et al*., 1995). Although composite accounts for the presence of different vegetation types, the composite vegetated surface does not exist in nature, as is depicted by the blended color of the panel marked 'composite' in figure 1.

A few of the AMIP II GCMs and some others account for the subgrid-scale heterogeneity using the 'mosaic' approach. In this approach, the heterogeneous grid box is characterized by different vegetation and soil types and their fractional area of coverage in the grid box (Koster and Suarez, 1992). This approach is depicted in the panel of figure 1 named 'mosaic'. The 'tiles' result from treating all of the bare soil portions as though they are juxtaposed, as are all of the deciduous trees, evergreen trees and shrubs. Separate surface heat and moisture balance equations are solved for each vegetation type contained within a GCM grid square and the resulting heat and moisture fluxes, which describe the coupling to the atmospheric boundary layer, are aggregated linearly. The turbulent diffusion in the boundary layer and above is then computed based on the grid-averaged surface flux of heat and moisture. The mosaic approach is employed, for example, in the GCMs used at the Goddard Institute for Space Studies (Rosenzweig and Abramopoulos, 1997), Laboratoire Météorologie Dynamique (Ducoudre *et al*., 1993), the Australian Bureau of Meteorology Research Centre (Desborough and Pitman, 1998), and the NASA/Goddard Seasonal to Interannual Prediction Project (Koster and Suarez, 1992). Many researchers, using either *in situ* data or high-resolution models as the basis for comparison, have carried out validations of the mosaic approach for GCMs (see, for example, Bringfelt, 1999; van den Hurk and Beljaars, 1996; Klink, 1995). The results of these evaluations generally show that the mosaic approach is an improvement over a composite or dominant approach, and that mosaic provides a reasonable approximation of the turbulent fluxes at the surface under many conditions.

2 Consensus of Results from GCM Studies

Using the land surface models described above, many GCM studies have been conducted to simulate the impact of LUC on climate. The majority of these studies have focused on deforestation and desertification. There have been several comprehensive reviews of GCM deforestation studies, compiled by, for example, Dickinson and Henderson-Sellers (1988), Shukla *et al*. (1990) and Hahmann and Dickinson (1999). There is general agreement among these studies about the basic processes which occur as a consequence of deforestation; however, the details and magnitudes differ substantially from study to study. These simulations conceptualize deforestation in terms of a conversion of forest into grassland. The interactions and feedback mechanisms involved as deforestation takes place are described below, with the aid of the schematic representation of figure 2. The two parallel loops in the schematic represent the feedbacks associated with the energy and hydrological cycles, and the box around the evaporation indicates the role of evapotranspiration in both cycles.

The feedback mechanism begins with the external forcing. As forested areas are converted to grassland, the albedo of the surface is increased, the surface roughness is decreased, and the ability of the underlying soil and vegetation canopy to hold water is also decreased. These are indicated in black ink by ‘Bright’, ‘Smooth’ and ‘Dry Veg’, respectively, in the figure, considered as the forcing in the simulations. In general, the deforestation results in a reduction of evaporation and precipitation and an increase of surface skin temperature (red colored ‘Evap’ and ‘Precip’, and blue colored ‘T surf’, respectively). This is accomplished through several paths. In the energy cycle loop, the increased surface albedo of the pasture lands leads to a decrease in the net surface solar radiation (red colored ‘Net Rad’), and so to a decrease in the energy available for evaporation and sensible heat flux. The decrease in surface roughness also contributes to the decrease in turbulent surface fluxes by reducing the mechanical sources of turbulence. In the hydrological cycle ‘loop’, the reduction in canopy and soil water capacity further serves to reduce the evapotranspiration, indicated as the inner loop of figure 2. As a result of the reduced evaporative cooling, the surface skin temperature increases, as shown in the outer loop in the figure. This temperature increase leads to an increased outgoing long wave radiation (blue colored ‘LW up’), which further depletes the net energy available at the surface. The reduced evaporation also results in a reduction of precipitation and the continuation of the canopy and soil drying cycle. The warmer surface leads to an increase in buoyancy but the decrease in mechanical turbulence and evaporation compensate and overcome this increase, resulting in a net decrease in vertical motion, indicated by ‘Rising Air’ in red along the inner-most loop in figure 2, and, therefore, a decrease in the moisture convergence into the region (red colored 'Moist Conv'). This serves to further reduce the precipitation and accelerate the drying and warming feedback cycle.

GCM simulations have also been performed to examine the combined effects of deforestation and doubling of carbon dioxide atmospheric concentrations (Costa and Foley, 2000). Both CO_2 increase and deforestation contribute to a warmer surface temperature. The competing effects on the hydrological cycle, however, were dominated by the deforestation, resulting in a decreased precipitation and evaporation. GCM studies have also investigated the relative role of different characteristics of a deforested region. Lean and Rowntree (1997) compared numerical experiments where deforestation alters only the albedo with experiments in which the albedo and surface roughness were altered. From these experiments they concluded that the albedo and roughness changes are comparable in their influence on the regional climate. In addition to the regional changes due to deforestation, GCM simulations also demonstrate its remote influence. Werth and Avissar (2002), in their study of the teleconnection patterns in European climate generated by Amazonian deforestation, suggest that planetary scale Rossby waves may indeed be excited due to processes that occur at the land surface, related to changes in landscape. Gedney and Valdes (2000) also found remote impacts of Amazon deforestation on the winter rainfall in the northeastern Atlantic and Western Europe, associated with the propagation of planetary waves.

The magnitude of the changes in climate due to deforestation differs substantially from model to model for comparable experiments. The reduction in precipitation ranges from 15 to 640 mm per year, the reduction in evaporation ranges from 25 to 500 mm per year and the range of increase in surface temperature is from 0.1 to 2.3°C (Lean and Rowntree, 1997). The studies showing the largest changes in precipitation do not correspond with those that report the largest changes in evaporation or surface temperature. The discrepancies among these GCM results are intimately related to a large extent to the role that cloud radiative feedbacks play in the particular model. The reduced precipitation is associated with a decrease in cloud cover, which leads to an increase in downward solar radiation and a decrease in downward long wave radiation. It is the net effect of this radiative feedback on the surface energy balance that varies both in magnitude and sign from model to model. The discrepancies among the GCM results are also related to other details of the GCM parameterizations. The magnitude of precipitation recycling (the partition between local and remote moisture sources of precipitation) in the various models, tied in large part to the closure assumption in the cumulus parameterization, is related to the discrepancies in rainfall reduction in a deforested region.

Another important consequence of anthropogenic LUC is desertification. GCM studies have shown that this LUC induces changes in the regional climate in much the same manner as does deforestation. The most extensively studied area of desertification is the Sahel-Sahara region (see, for example, Nicholson *et al*., 1998). Charney's albedo feedback hypothesis (Charney, 1975) postulates that an increase in surface albedo would increase radiative losses over the Sahara and would enhance the negative net radiation balance of the desert and adjacent Sahel. GCM experiments on the roles of albedo, evapotranspiration, and roughness have generally concluded that a positive feedback exists, and includes a reduction in rainfall which further alters the vegetation and soil to promote desertification (see, for example, Sud and Molod, 1988 and Xue and Shukla, 1993). GCM studies have also shown that the Sahelian drought of the 1970s, although initiated by anomalous sea-surface temperatures was perpetuated by Charney-type local land-atmosphere interactions (Giannini *et al*., 2003). Similarly, precipitation anomalies associated with ocean temperatures, in conjunction with agricultural practices, resulted in the initiation of local land-atmosphere feedbacks that led to the dust-bowl event of the 1930s (Schubert *et al*., 2004). GCM studies have also demonstrated that large-scale desertification in the northeast area of Brazil results in a weaker hydrological cycle (Sud and Fennessy, 1982,1984) and that, in addition, results in an increase in precipitation over the adjacent ocean areas (Oyama and Nobre, 2004). As with GCM studies of deforestation, there are discrepancies among GCM simulations of desertification in the northeast of Brazil. For example, Dirmeyer and Shukla (1996) concluded that a change of the region's vegetation to a semi-desert vegetation would not affect the regional hydrological cycle.

All of these modeling studies provide the means to understand the physical mechanisms and feedbacks involved in the communication of anthropogenic activity to the regional and global climate. The conclusions drawn from these studies rely on the details of the model parameterizations and are sensitive to the choice of models. The lack of agreement among model results is an indication of the inaccuracies in model parameterizations that still require close inspection.

III. A Recent Development: 'Extended Mosaic'

1 Limitations of Previous Techniques

One of the aspects of the land-atmosphere coupling techniques that represents a limitation is related to the level at which the boundary layer is assumed to be homogeneous. Mosaic, composite and dominant all assume that the atmospheric properties are horizontally homogeneous at or below the surface layer height. Observational and modeling studies (Claussen, 1995; Mahrt, 2000 and articles cited therein), however, have shown that the direct influence of the surface heterogeneities extends vertically in the atmosphere up to a level that may be above the surface layer (which is nominally 50 m above the ground) and within the planetary boundary layer (on the order of 1 km above the ground). Early studies of the vertical influence of the land surface heterogeneities were conducted by Wieringa (1986), where he defined the 'blending height' as the level inside the planetary boundary layer above which the flow becomes horizontally homogeneous in the absence of other influences. For horizontal scales of heterogeneity of the order of 50 to 100 km or larger that characterize part of the globe, this would imply a blending height of 500 m to 1 km, which is of the order of the planetary boundary layer height. A comprehensive survey of blending height estimates under different atmospheric conditions was presented by Mahrt (1996), where he reported that the blending height can be as high as the height of the planetary boundary layer (PBL), or even higher for an unstable atmosphere under the influence of strong surface heating.

Observational evidence exists which supports the scaling arguments that suggest that the blending height may extend well into the PBL. Segal *et al*. (1989) show, using aircraft measurements of temperature and humidity at four levels in the atmosphere over the boundary between an irrigated and a dry crop area, that the contrast between the wet, cool air over the irrigated area and the dry, warm air over the dry area extends up to at least 440 m above the surface. These observations would suggest that the blending height is somewhere above 440 m. The presence of an “elevated large scale blending height” can also be inferred from lidar measurements of the mixed layer height taken in the vicinity of Nashville, Tennessee, spanning the interface between a forested and an agricultural area. The mixed layer heights over the different terrain with patch sizes of ~30 km were shown to differ by up to 400 m (Angevine *et al*., 2003).

The existence of a blending height on larger scales is also demonstrated by a study that uses radiosonde data from the 1994 field observations obtained during the Boreal Ecosystem Atmospheric Study (BOREAS) (Salmun *et al*., 2004). The data used in this analysis were from temporally concurrent measurements (daytime or afternoon), taken over a wide enough range of surface types and separated by distances comparable to a GCM grid size. Blending heights were observed in more than 80 % of the vertical soundings from the seven locations that were analyzed, and on average over 50 % of the estimated blending heights were found at altitudes above 1 km.

Evidence that the blending height may be of the same order as the planetary boundary layer height has implications for the different techniques used to capture subgrid scale heterogeneity in a GCM. The composite approach does not allow for the direct propagation of the independent characteristics of each vegetation type into the atmosphere at all. The ‘mosaic’ technique only accounts for the influence of land surface heterogeneities within the surface layer. The limits on the vertical influence of surface heterogeneities imposed by these techniques may well constitute an important limitation to capturing the effectiveness of the communication between the land surface heterogeneity and the atmosphere (Mahrt, 2000).

2 The Extended Mosaic Algorithm and its Impact on the Modeled Climate

The technique called ‘Extended Mosaic’ (EM) presented in Molod *et al*. (2003) is designed to allow the subgrid scale interactions between the land surface and the atmosphere to extend vertically. This is depicted schematically in figure 3, where the lowest level is identical to the representation of a grid square using the mosaic approach depicted in figure 1. Figure 3 illustrates that in the EM technique the heterogeneity at each model level, LM, LM-1, etc., is conceptualized in terms of the same tiles that characterize the surface. The subgrid scale variability of the surface is modeled by computing energy and moisture transfers in the surface layer and soil separately for each ‘tile’ that makes up the mosaic, as with the standard mosaic technique. This idea is extended upwards in EM by computing energy and moisture transfers in the turbulent layer above separately for each ‘tile’ as well. The net change in temperature and moisture (and passive tracers) is aggregated to compute a GCM grid average at *all levels* in the atmosphere. Implementation of this scheme in a GCM allows the level of the blending height to be *diagnosed as a result* of the behavior of the turbulent boundary layer over each different vegetation type, rather than be *chosen a priori*. The model blending height computed using extended mosaic, its variability and behavior, was analyzed in Molod *et al*. (2003). Extended mosaic therefore addresses a limitation of previously existing techniques, and has been shown in Molod *et al*. (2004) to have an important impact on the simulated climate in global models. Two 10-year long simulations were performed with the GEOS GCM to evaluate the impact on the resulting climate of using the EM technique rather than a standard mosaic technique. The results of these side-by-side simulations showed statistically significant differences on local and global scales.

The impact on the local boundary layer structure was illustrated by elucidating a boundary layer eddy diffusion feedback mechanism present in several regions around the globe. This feedback is illustrated schematically in figure 4. The initiation of the feedback, indicated by ‘More turb’ in the figure, is the enhancement of the eddy diffusion in EM relative to M as a direct result of the change in technique. This enhanced eddy diffusion of heat and moisture generates higher temperatures and humidity aloft in the boundary layer (black colored ‘higher T bl, q bl’). In the eastern US , the circular path on the left of figure 4, the higher boundary layer temperature (‘T bl’) resulted in a lower relative humidity at those levels, and the suppression of the precipitation (red colored ‘Rel Hum’ and ‘Precip’, respectively). The lower precipitation resulted in drier soils and less evaporation (red colored ‘Soil Wat’ and ‘Evap’), which acted to warm the canopy temperatures, denoted by ‘T surf’ in blue. The warmer skin temperatures, in turn, generated higher sensible heat flux and higher eddy diffusion (blue ‘Turb’ in the figure). This completed a positive feedback loop.

The enhanced eddy diffusion and subsequent increase of boundary layer temperature and humidity results in a pattern of opposite sign over a region in northern China and Mongolia, shown by the circular path on the right of figure 4. Over this region, the temperature aloft (‘T bl’), canopy temperature (‘T surf’) and sensible heat fluxes (denoted as a decrease in ‘Turb’ for turbulent fluxes, in the figure) were all lower in EM, and the precipitation and evaporation were higher (blue colored ‘Evap’ and ‘Precip’). In this region, the presence of a deciduous forest and the dominant role played by the moisture diffusion results in a higher relative humidity aloft (blue ‘Rel Hum’), and enhances the precipitation in the EM simulation. This initiates a positive feedback in the opposite sense, with enhanced precipitation and wetter soils resulting in an increase in evaporation, and therefore a cooling of the surface (a further decrease in ‘T surf’). The remote impact on the global climate was demonstrated by the strengthening in the EM simulation (relative to the standard mosaic simulation) of a teleconnection pattern known as the Pacific-North-America (PNA) pattern of variability. The possible influence of the land surface hydrology on the amplitude of the PNA has been reported by Trenberth *et al*. (1998) in a study based on observations and model results.

3 Strength of Land-Atmosphere Coupling

The comparison between the two modeling techniques discussed above, when viewed as a difference in the amount of subgrid scale variability that is allowed to propagate through the climate system by the different models, gives an indication of the response to a perturbation in the character of the underlying land surface. An indicator of the extent to which a perturbation in the character of the land surface (through anthropogenic LUC, for instance) will affect the global climate is the strength of the coupling between the land surface and the atmosphere.

Koster *et al*. (2002) (hereafter K02) defined a measure of the strength of the land-atmosphere coupling and studied how it varies among different GCMs. The definition essentially identifies the contribution of the land-atmosphere coupling to the total variability of the GCM climate.

K02 designed a series of experiments to isolate the contribution of the variability in a GCM climate due to the land-atmosphere coupling from the total model variability. They ran two ensembles for each GCM they examined, one in which the variability due to ocean and solar forcing, atmospheric internal variability and land-atmosphere coupling were allowed, and one in which only solar and ocean forcing and atmospheric internal variability were allowed. They examined the differences between these ensembles to deduce the contribution of the land to the total variability, interpreted as the strength of the land-atmosphere coupling.

The measure of the coupling strength using the evaporation field is defined in K02 by the quantity:

$$\Omega_E = \frac{n\sigma_{\hat{E}}^2 - \sigma_E^2}{(n-1)\sigma_E^2} \quad ,$$

where n is the total number of ensemble members, σ_E^2 is the variance of the evaporation E across all ensemble members and all time periods and $\sigma_{\hat{E}}^2$ is the variance of Ê, the ensemble mean. According to this definition, if each ensemble member is identical, then $\sigma_E^2 = \sigma_{\hat{E}}^2$ and $\Omega_E = 1$, and, conversely, if all the members of the ensemble are uncorrelated then $\sigma_E^2 = n\sigma_{\hat{E}}^2$ and $\Omega_E = 0$. A similar definition can be made for the precipitation field. For the ensemble in which the variability due to the land-atmosphere coupling is suppressed, a finding that the ensemble members are highly correlated would mean that there is little variability due to the ocean and solar forcing and little atmospheric internal variability. The implication would be that the land surface provides the variability that exists in the original ensemble.

Following this framework of analysis, we construct an ensemble for the EM technique and one for the standard mosaic technique (hereafter M) based on our 10-year simulations driven by climatological sea surface temperatures. We regard each of our 10-year simulations as a 10 member ensemble of 1-year simulations. Because the external forcing for these simulations (solar and oceanic) is the same for every year of our simulations, we can regard them as 10 repetitions of the same experiment with 10 different sets of initial atmospheric and land surface conditions. We assume that the correlations between the initial conditions for each of these repetitions are small enough to be neglected for the purpose of constructing an ensemble.

Although we cannot directly isolate the contribution of the land-atmosphere coupling to the total variability in the same manner as K02 based on the design of our experimental ensemble, we can infer that contribution from our experiments if we examine the differences between EM and M. In our ensemble, if the sea surface temperature alone governs the behavior of the evaporation, then all the time series of evaporation from the different ensemble members would be nearly perfectly correlated and the Ω_E based on our ensemble should be nearly 1, or that $(1-\Omega_E)$ is nearly 0. To the extent that atmospheric variability and the land boundary condition play a role in determining the outcome of the evaporation in each simulation, the time series would be less correlated and $(1-\Omega_E)$ would be larger. In order to distinguish between the contributions of the land surface from the atmospheric internal variability, we assume that the magnitude of the natural variability in the EM and in the M ensembles is not substantially different, and we examine differences between $(1-\Omega_E)$ from the EM and M ensembles.

Global maps of the EM-M difference of $(1-\Omega_E)$ for evaporation and of $(1-\Omega_P)$ for precipitation are shown in figure 5 a and b, respectively. This estimation of the land-atmosphere coupling strength reveals several regions where the EM-M difference in $(1-\Omega_E)$ is positive (values corresponding to orange and red shading in particular). The large area in the central United States observed in both panels of figure 5 indicates regions where the land surface in EM exerts more influence on the variability of the evaporation and precipitation than in M. Other regions where the EM-M difference in $(1-\Omega_E)$ is positive appear clearly in areas of southern Africa, a limited area over Sahel, and over central and north-east region of Australia. Figure 5 also shows areas where the strength of the coupling is weakened in EM relative to M, indicated by the blue regions over land in the figures. The largest area of negative values of the EM-M difference in $(1-\Omega_E)$ is found over north-central Canada, and smaller areas are dispersed over other parts of the globe, most notably over central Europe and Asia. Most of the regions for which the coupling is strengthened coincide with regions identified as 'hot spots' in a study reported by Koster *et al*. 2004 in which experiments with several GCMs were conducted to quantify the strength of the land-atmosphere coupling in each model as well as averaged across all models. The results of our simulations therefore indicate that in a model using EM the strength of the land-atmosphere coupling has been increased in many regions, from which we understand that EM would simulate an increased response relative to M to a change in the character of the land surface.

IV. Concluding Remarks

In this article we have addressed some of the issues involved in understanding and predicting the impact of anthropogenic land use change (LUC) on regional and global climate and climate change. To a large extent, our understanding of these issues comes from studies conducted with General Circulation Models (GCMs). We presented a description of the physical mechanisms involved in how deforestation and desertification impact climate from a consensus of GCM studies. A newly developed technique to model the land-atmosphere coupling in a GCM was discussed, which addresses some existing limitations in the models and may affect the results of LUC studies. In support of this notion, we reviewed a study conducted using the new technique which revealed the presence of a boundary layer eddy diffusion feedback mechanism that was not present in simulations with the standard technique. In addition, a measure of the relative strength of the land-atmosphere as simulated by the new technique versus the standard mosaic technique was presented which showed that the land-atmosphere coupling was strengthened over a region in the U.S Central Plains. This region coincides roughly with one of the 'hot spots' identified by the study of Koster *et al*. 2004, as regions where the atmosphere is strongly influenced by the land surface.

In our discussion, we stressed that our understanding of the physical mechanisms involved in the impact of anthropogenic land use change on the climate system is tied to the particulars of the land-atmosphere coupling in GCMs. Our focus is the manner in which interactions at the land boundary are communicated higher up into the atmosphere, an issue which is specifically addressed by the extended mosaic (EM) technique under discussion here. We argue that this technique can provide new insight into understanding how LUC impacts climate. We illustrate this point by examining the mechanisms for the LUC impact laid out in the schematic of figure 2, which is based on a consensus of models without EM. The particular causal link for our illustration is the decrease of evaporation due to the decreased roughness during deforestation. An element of the boundary layer feedback mechanism found in the study comparing EM to a standard mosaic (figure 4) is the possibility that intensifying the turbulence can lead to *either* an increase *or* a decrease in the intensity of the hydrological cycle, depending on the character of the underlying surface. This suggests that in a deforestation simulation using EM the impact of the change in the intensity of the boundary layer turbulence due to the lowered surface roughness *may* result in an *increase* in evaporation if the surface is wet enough. If, for example, at the early stages of deforestation the surface is moist, is it possible to enhance the evaporation process despite the removal of the trees. As deforestation increases and the other stresses on the moisture become more important, the drying of the surface may result in a reversal of the causality, whereby a decreased roughness will result in a decreased evapotranspiration. The use of EM allows for the possibility of this alternative response, which may be relevant for investigating the impact of LUC such as deforestation.

We postulate that any GCM that uses the EM technique to couple the land surface model and the atmospheric turbulence scheme has the potential to improve our ability to simulate the land-atmosphere exchanges. This postulate is based (a) on the improved ability to capture the subgrid scale interactions between the land surface and the atmosphere which is part of the design of the EM technique, and (b) on comparisons between EM and the standard mosaic technique which reveal a stronger land-atmosphere coupling in regions of interest and a boundary layer feedback mechanism. Using EM in a GCM may result in improved predictions of the influence of anthropogenic land use change on the climate. We plan to conduct deforestation experiments with a GCM that includes EM to evaluate this assertion, and advocate the use of the EM technique in other GCMs that will be used for the ongoing deforestation studies that will contribute to our understanding of how anthropogenic LUC will impact the climate.

Acknowledgments

The first author is grateful for the support provided by the Gender Equity Project

References

Angevine, W.M., White, A.B., Senff, C.J., Trainer, M., Banta, R.M. and **Ayoub. M.A.** 2003: Urban-rural contrasts in mixing height and cloudiness over Nashville in 1999. *Journal of Geophysical Research* 108 (D3), 10.1029/2001JD001061.

Bringfelt, B. 1999: A new land-surface treatment for HIRLAM - Comparisons with NOPEX measurements. *Agricultural Forest Meteorology* 98-9, 239-256.

Charney, J.G. 1975: Dynamics of deserts and drought in the Sahel. *Quart. J. Roy. Meteor. Soc*. 101, 193-202.

Claussen, M. 1995: Flux aggregation at large scales. On the limits of validity of the concept of blending height. *Journal of Hydrology* 166, 371-382.

Costa, M.H. and **Foley, J.A.** 2000: Combined effects of deforestation and doubled atmospheric CO2 concentrations on the climate of Amazonia. *J. Climate* 13, 18-34.

Cotton, W.R. and **Pielke. R.A.** 1992: *Human Impacts on Weather and Climate*, Cambridge University Press, 288pp.

Desborough, C.E. and **Pitman, A.J.** 1998: The BASE land surface model. *Global and Planetary Change* 19,3-18.

Dickinson, R. E. and **Henderson-Sellers, A.** 1988: Modelling tropical deforestation: A study of GCM land-surface parameterizations. *Quart. J. Roy. Meteor. Soc.* 114, 439-462.

Dickinson, R., Henderson-Sellers, A., Kennedy, P. and **Wilson, M.** 1986: Biosphere-Atmosphere Transfer Scheme (BATS) for NCAR community climate model. *Technical Note TN 275+STR*, 69pp. National Center for Atmospheric Research, Boulder, Colorado.

Dirmeyer, P.A. and **Shukla J.** 1996: The effect on regional and global climate of expansion of the world's deserts. *Quart. J. Roy. Meteor. Soc.* 122, 451-482.

Ducoudre, N. I., Laval, K. and **Perrier, A.** 1993: SECHIBA, a new set of parameterizations of the hydrologic exchanges at the land-atmosphere interface within the LMD atmospheric general circulation model. *J. Climate* 6, 248-273.

Durieux, L., Machado, L.A.T. and **H. Laurent, H.** 2003: The impact of deforestation on cloud cover over the Amazon arc of deforestation. *Remote Sensing of the Environment* 86: 132-140.

Gallo, K.P., Owen, T.W., Easterling, D.R. and **Jamason, P.F.** 1999: Temperature trends of the US historical climatology network based on satellite-designated land use/land cover. *J. Climate* 12, 1344-1348.

Gates, W. L. ed. 1995: The proceedings of the First International AMIP Scientific Conference. WCRP-92, WMO/TD-No. 732. *World Climate Research Programme*, World Meteorological Organization, Geneva, 532pp.

Gedney, N. and **Valdes, P.J.** 2000: The effect of Amazon deforestation on the N. Hemisphere circulation and climate. *Geophys. Res. Letters* 27, 3053-3056.

Giannini, A., Saravanan, R. and **Chang, P.** 2003: Oceanic forcing of Sahel rainfall on interannual to interdecadal time scales. *Science* 302, 1027-1030.

Hahmann, A. and **Dickinson, R. E.** 1997: RCCM2/BATS Model over tropical South America: applications to tropical deforestation. *J. Climate* 10, 1944-1964.

Intergovernmental Panel on Climate Change (IPCC) 2001: *Climate Change 2001: Synthesis Report: Contribution of working groups I, II and III to the Third Assessment Report*. Cambridge Press.

Kalnay, E. and **Cai, M.** 2003: Impact of urbanization and land use change on climate. *Nature* 423, 528-531.

Klink, K. 1995: Surface aggregation and subgrid-scale climate. *Int. J. Climatology* 15, 1219–1240.

Koster, R.D. and the **GLACE Team**: **Dirmeyer, P.A., Guo, Z., Bonan, G., Chan, E., Cox, P., Gordon, C.T., Kanae, S., Kowalczyk, E., Lawrence, D., Liu, P., Lu, Ch-H., Malyshev, S., McAvaney, B., Mitchell, K., Mocko, D., Oki, T., Oleson, K., Pitman, A.J., Sud, Y.C., Taylor, C.M., Verseghy, D., Vasic, R., Xue, Y.** and **Yamada, T.** 2004. Regions of strong coupling between soil moisture and precipitation. *Science* 305, 1138-1140.

Koster, R.D., Dirmeyer, P.A., Hahmann, A., Ijpelaar, R., Tyahla, L., P. Cox, P. and **Suarez, M.J.** 2002: Comparing the Degree of Land-Atmosphere Interaction in Four Atmospheric General Circulation Models. *J. Hydrometeorology* 3, 363-375.

Koster, R.D. and **M. J. Suarez, M.J.** 1992: Modeling the land surface boundary in climate models as a composite of independent vegetation stands. *J. Geophysical Research* 97, 2697-2715.

Lean, J. and **Rowntree, P.R.** 1997: Understanding the Sensitivity of a GCM Simulation Amazonian Deforestation to the Specification of Vegetation and Soil Characteristics. *J. Climate* 10, 1216-1235.

Mahfouf, J-F., Manzi, A.O., Noilhan, J., Giordani, H. and **Deque, M.** 1995: The land surface scheme ISBA within the Météo -France climate model ARPEGE. Part I. Implementation and preliminary results. *J. Climate* 8, 2039-2057.

Mahrt, L. 1996: The bulk aerodynamic formulation over heterogeneous surfaces. *Boundary-Layer Meteorology* 78, 87-119.

Mahrt, L. 2000: Surface heterogeneity and vertical structure of the boundary layer. *Boundary-Layer Meteorology* 96 (1-2), 33-62.

Millan, M. M., Estrela, M. J., Sanz, M. J., Mantilla, E., Martín, M., Pastor, F., Salvador, R., Vallejo, R., Alonso, L., Gangioti, G., Ilardia, J. L., Navazo, M., Albizuri, A., Artiñano, B., Ciccioli, P., Kallos, G., Carvalho, R. A., Andrés, D., Hoff, A., Werhahn, J., Seufert, G., and **Versino, B.** 2005**:** Climatic Feedbacks and Desertification: The Mediterranean Model. *J. Climate* 18 (5), 684-701.

Molod, A., Salmun, H. and **Waugh, D.W.** 2004: The impact on a GCM climate of an extended mosaic technique for the land-atmosphere coupling. *J. Climate* 17 (20), 3877–3891.

Molod, A., Salmun, H. and **Waugh, D.W.** 2003: A new look at modeling surface heterogeneity: extending its influence in the vertical. *J. Hydrometeorology* 4, 810-825.

Nicholson, S.E., Tucker, C.J. and **Ba, M.B.** 1998: Desertification, drought and surface vegetation: an example from the West African Sahel. *Bull. Amer. Meteor. Soc.* 79, 815-29.

Oyama, M.D. and **Nobre, C.A.** 2004: Climatic Consequences of a Large-Scale Desertification in Northeast Brazil: A GCM Simulation Study. *J. Climate* 17, 3203-3213.

Pan, H-L. and **Mahrt, L.** 1987: Interaction between soil hydrology and boundary layer development. *Boundary-Layer Meteorology* 38, 185-202.

Pielke, R.A. Sr., Marland, G., Betts, R.A., Chase, T.N., Eastman, J.L., Niles, J.O., Niyogi, D. and **Running, S.W.** 2002: The influence of land use change and landscape dynamics on the climate system: relevance to climate change policy beyond the radiative effects of greenhouse gases. *Phil. Trans. Roy. Soc. London A* 360, 1-15.

Pielke, R.A.Sr., Walko, R.L., Steyaert, L.T., Vidale, P.L., Liston, G.E., Lyons, W.A. and **T. Chase, T.** 1999: The influence of anthropogenic landscape changes on weather in south Florida. *Monthly Weather Review* 127, 1663-1673.

Pitman, A.J. 2003: ReviewThe evolution of, and revolution in, land surface schemes designed for climate models. *Int. J. Climatology* 23, 479–510.

Randall, D. 2000: General circulation model development: past, present and future. Academic Press, 807pp.

Ray, D.K., Nair, US , Welch, R.M., Su, W. and **T. Kikuchi, T.** 2001: Influence of land use on the regional climate of southwest Australia. *EOS Transactions* 82 (20). AGU Spring 2001, San Francisco, CA.

Rosenzweig, C. and **Abramopoulos, F.** 1997: Land-surface model development for the GISS GCM. *J. Climate* 10, 2040-2054.

Salmun, H., Molod, A. and **Huang, L.** 2004: GCM-scale blending heights from the BOREAS observations. *EOS Transactions* 87 (17). Joint Assembly, Montreal, Canada, May 2004.

Schubert, S.D., Suarez, M.J., Pegion,P.J., Koster, R.D. and **Bacmeister, J.T.** 2004: On the cause of the 1930's dust bowl. *Science* 303, 1855-1859.

Segal, M., Schreiber, W., G. Kallos, G., Pielke, R.A., Garrat, J.R., Weaver, J., Rodi, A. and **Wilson,** J. 1989: The impact of crop areas in northeast Colorado on midsummer mesoscale thermal circulations. *Monthly Weather Review* 117, 809-825.

Shukla, J., Nobre, C.A. and **Sellers, P.J.** 1990: Amazonia deforestation and climate change. *Science* 247: 1322-1325.

Sud, Y.C. and **Molod, A.** 1988: A GCM simulation study of the influence of Saharan evapotranspiration and surface-albedo anomalies on July circulation and rainfall. *Mon. Wea. Rev.* 116: 2388-2400.

Sud, Y.C. and **Fennessy, M.** 1984: Influence of evaporation in semi-arid regions on the July circulation: a numerical study. *J. Climatology* 4: 383-398.

Sud, Y.C. and **Fennessy, M.** 1982: A study of the influence of surface albedo on July circulation in semi-arid regions using the GLAS GCM. *J. Climatology* 2: 105-125.

Trenberth, K.E., Branstator, G.W., Karoly, D., Kumar, A., Lau, N-C. and **C. Ropelewski, C.** 1998: Progress during TOGA in understanding and modeling global teleconnections associated with tropical sea surface temperatures. *J. Geophysical Research* 103(C7), 14291-14324.

van den Hurk, B.J.J.M. and **Beljaars, A.C.M.** 1996: Impact of some simplifying assumptions in the new ECMWF surface scheme. *J. Applied Meteorology* 35, 1333-1343.

Verseghy, D.L., McFarlane, N.A. and **Lazare, M.** 1993: CLASS - A Canadian land surface scheme for GCMs, II. Vegetation model and coupled runs. *Int. J. Climatology* 13, 347-370.

Viterbo, P. and **Beljaars, A.C.M.** 1995: An Improved Land Surface Parameterization Scheme in the ECMWF Model and its Validation. *J. Climate* 8, 2716-2748.

Werth, D. and **Avissar, R.** 2002: The local and global effects of Amazon deforestation. *J. Geophysical Research* 107(D20), 10.1029/2001JD000717.

Wieringa, J. 1986: Roughness-dependent geographical interpolation of surface wind speed averages. *Quar. J. Roy. Meteor. Soc.* 112, 867-889.

Xue, Y. and **Shukla, J.** 1993: The influence of land surface properties on Sahel climate: Part I. Desertification. *J. Climate* 6: 2232-2245

Xue, Y., Sellers, P.J., Kinter III, J.L. and **Shukla, J.** 1991: A simplified biosphere model for global climate studies. *J. Climate* 4, 345-364.

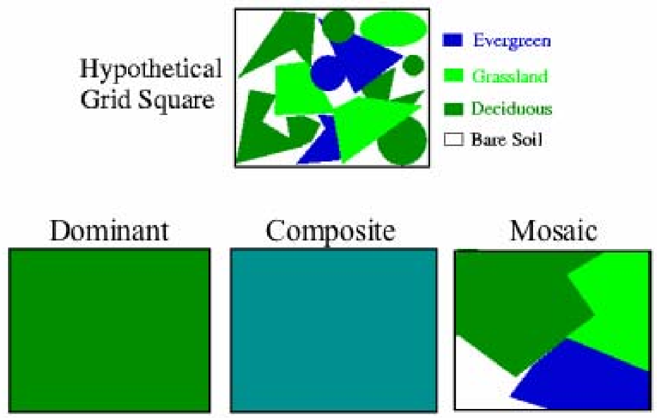

Figure 1 Schematic of the dominant, composite and mosaic techniques. The jagged shape of the tiles in the mosaic panel signifies an arbitrary shape, and the juxtaposition of tiles is not relevant.

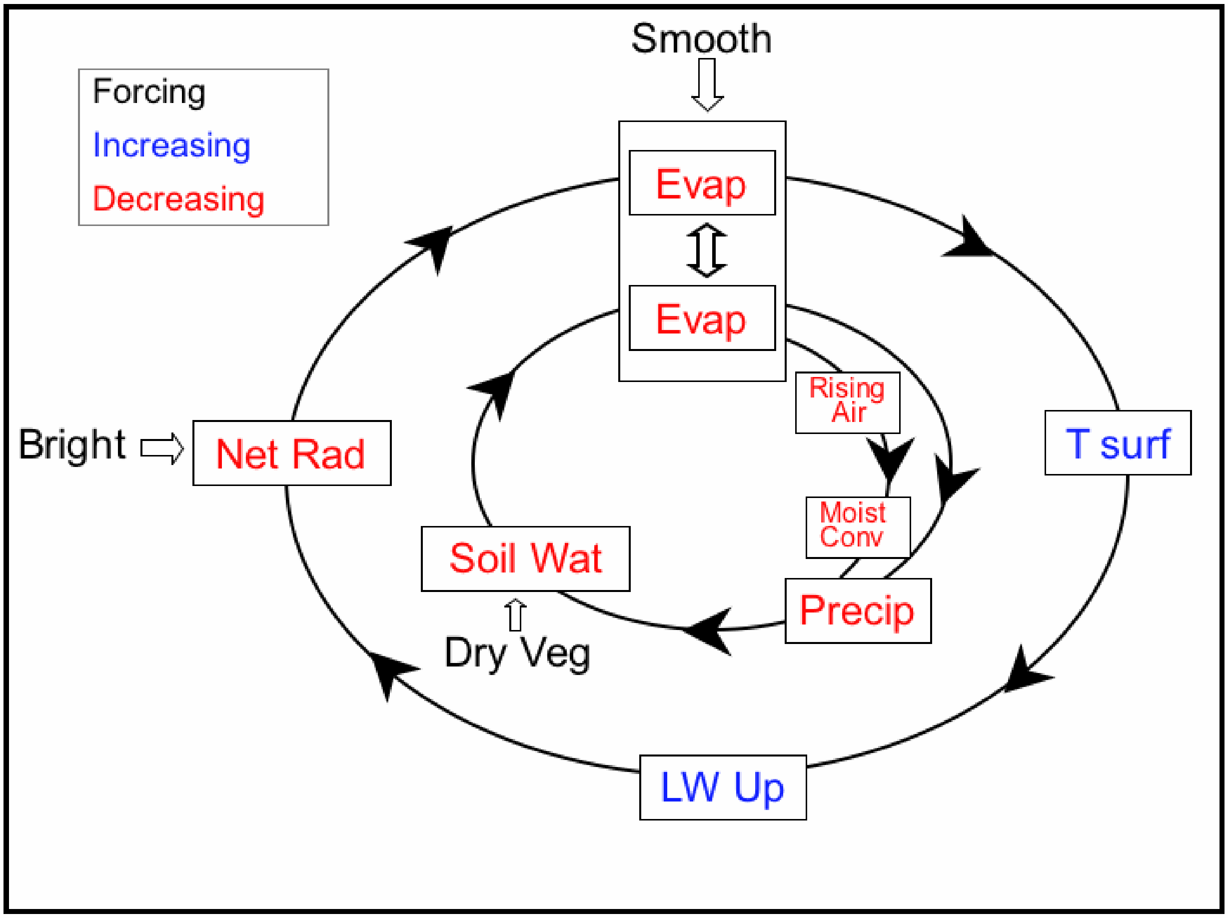

Figure 2 Schematic of the feedback mechanisms involved in deforestation, as described by GCM simulations. The symbols in the schematic are defined as follows: Soil Wat and T surf are the soil moisture and the surface temperature, respectively; Net Rad and LW Up are net surface solar radiation and the outgoing long wave radiation, respectively; Evap and Precip are the evaporation and the precipitation, respectively; and Moist Conv is the moisture convergence into the region.

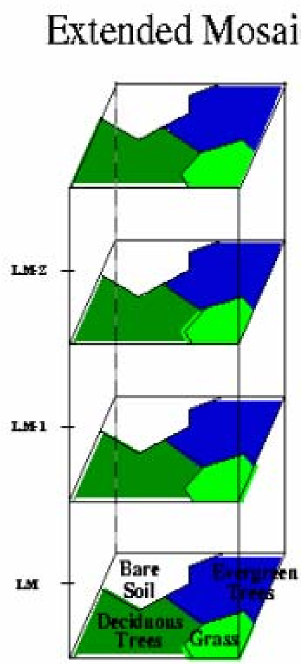

Figure 3 Schematic of the extended mosaic technique. The vertical axis indicates the GCM model levels, where LM is the lowest level and the level number decreases as we ascend in the column.

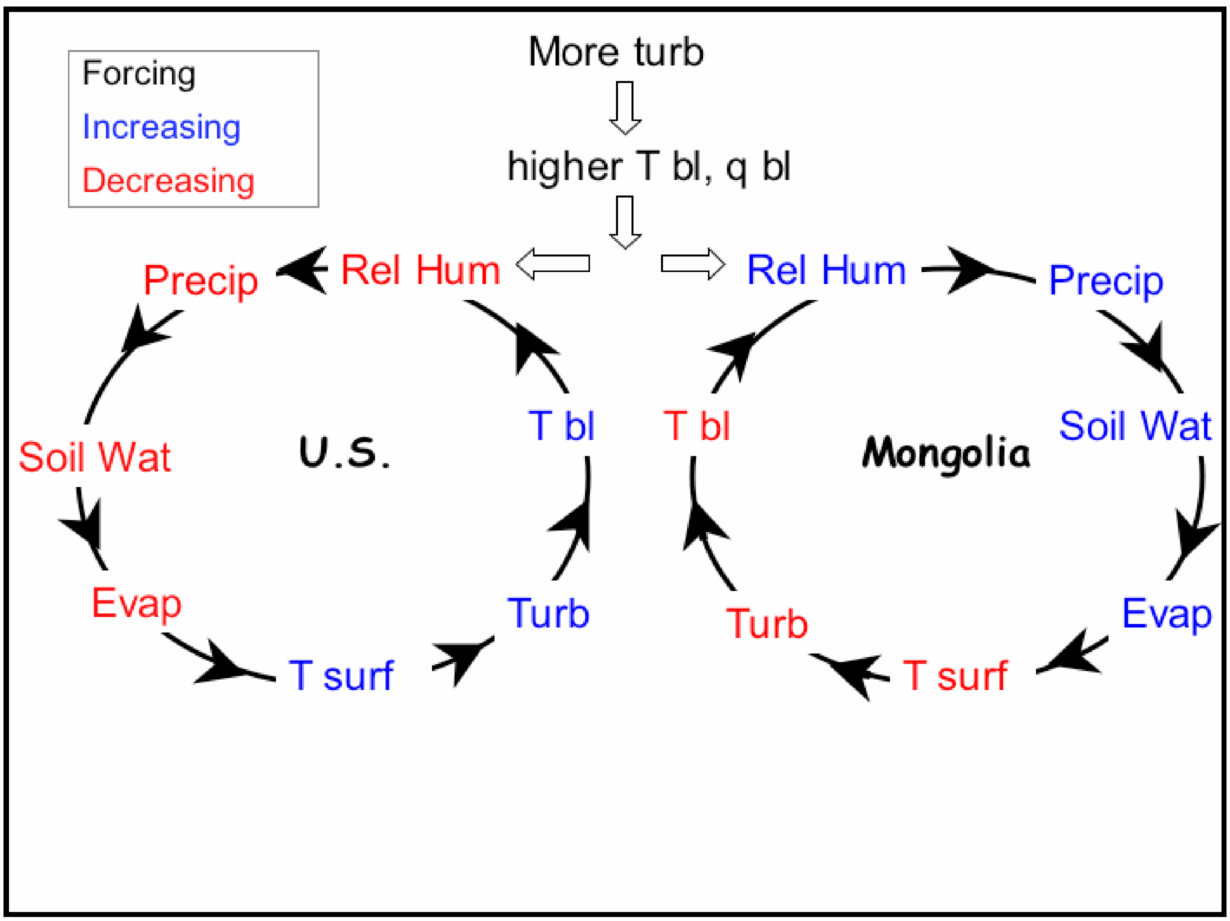

Figure 4 Schematic of the boundary layer eddy diffusion feedback mechanism due to using EM in GCM simulations performed by Molod *et al*. 2004. The manifestation of this feedback in the summertime over the eastern U.S. is shown on the left of the figure and its manifestation over an area of northern Mongolia on the right. Both loops indicate the positive feedback, but of opposite sense depending on local characteristics, which results from the enhancement of diffusion of heat and moisture when using EM. In the schematic, Soil Wat, T surf, T bl and Turb are used to denote soil moisture, surface (or canopy) temperature, boundary layer temperature aloft and eddy diffusion, respectively.

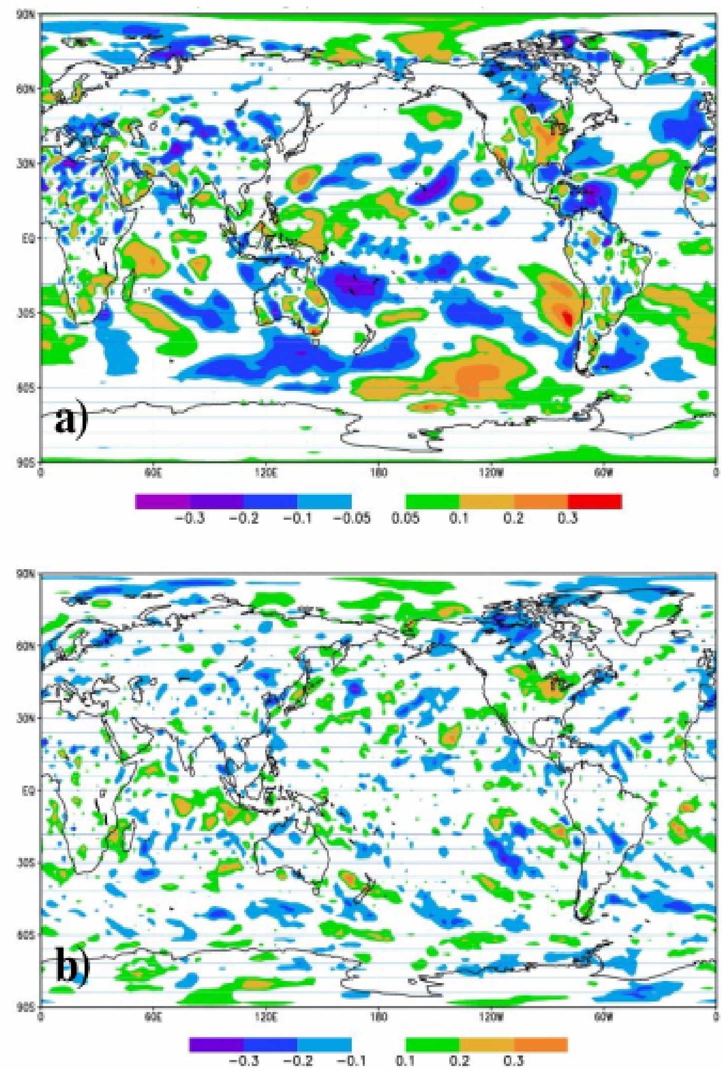

Figure 5 (a) EM -M difference of (1- Ω_E) and (b) EM-M difference of (1- Ω_P), measures of the strength of the land-atmosphere coupling. Large positive values, such as seen in the central US, indicate a stronger coupling in EM.